Contribution from the Laboratoire de Synthèse et d'Electrosynthèse Organométallique, Associé au CNRS (UA 33), Faculté des Sciences "Gabriel", Université de Bourgogne, 6 Boulevard Gabriel, 21100 Dijon, France, Department of Chemistry, University of Houston, Houston, Texas 77204-5641, Laboratoire de Chimie Physique Générale, Faculté des Sciences, Université Mohammed V, Rabat, Morocco, and Laboratoire de Minéralogie et Cristallographie Associé au CNRS (URA 809), Université de Nancy I, BP 239, 54506 Vandoeuvre-les-Nancy, France

Synthesis and Spectroscopic and Electrochemical Characterization of Ionic and σ-Bonded Aluminum(III) Porphyrins. Crystal Structure of Methyl(2,3,7,8,12,13,17,18-octaethylporphinato)aluminum(III), (OEP)Al(CH_3)

R. Guilard,*[1a] A. Zrineh,[1a,b] A. Tabard,[1a] A. Endo,[1c] B. C. Han,[1c] C. Lecomte,[1d] M. Souhassou,[1d] A. Habbou,[1d] M. Ferhat,[1b] and K. M. Kadish*[1c]

Received April 20, 1990

The synthesis and characterization of 10 different ionic and σ-bonded aluminum(III) porphyrins are reported. These compounds were studied by mass spectrometry and IR, UV-visible, and ^1H NMR spectroscopy as well as by electrochemistry. The spectroscopically investigated compounds are represented by (P)AlCl an (P)Al(R), where P is the dianion of tetraphenylporphyrin (TPP) or octaethylporphyrin (OEP) and R is CH_3, n-C_4H_9, C_6H_5, or C_6F_4H. The molecular structure of (OEP)Al(CH_3) was determined by X-ray diffraction and provides the first structural data for an aluminum porphyrin complex. The Al(III) atom in (OEP)Al(CH_3) is pentacoordinated and is located 0.465 (1) Å from the mean nitrogen plane. The electrochemically investigated compounds are represented by (P)AlCl and (P)Al(R), where P is OEP or TPP and R is CH_3, n-C_4H_9, or C_6H_5. An overall mechanism for the oxidation and reduction of each derivative is presented, and data for the σ-bonded complexes are compared to results obtained under the same experimental conditions for oxidation and reduction of (P)M(R), where M = Ga, In, or Tl.

Introduction

Numerous gallium,[2-8] indium,[2-6,9-19] and thallium[2-5,20,21] metalloporphyrins with ionic or σ-bonded axial ligands have been synthesized and spectroscopically or electrochemically characterized. These group 13 compounds may be represented as (P)M(R) or (P)MX, where P is the dianion of a given porphyrin ring, X is an anionic ligand, R is a σ-bonded alkyl or aryl group, and M is Ga(III), In(III), or Tl(III). Aluminum metalloporphyrins with σ-bonded axial ligands are also known,[22-26] but far less spectroscopic data are available for these compounds, which are highly photosensitive. In fact, the only Al(III) σ-bonded derivatives reported in the literature are (TPP)Al(CH_3) and (TPP)Al(C_2H_5), where TPP is the dianion of tetraphenylporphyrin.

In this present paper, we report the synthesis, spectroscopic characterization, and electrochemistry of 10 different Al(III) porphyrins. The investigated compounds are represented by (P)AlCl and (P)Al(R), where P is the dianion of octaethylporphyrin (OEP) or tetraphenylporphyrin (TPP) and R is CH_3, n-C_4H_9, C_6H_5, or C_6F_4H. Each compound was characterized by mass spectrometry and IR, UV-visible, and ^1H NMR spectroscopy as well as by electrochemistry.

No electrochemistry of a σ-bonded aluminum porphyrin has ever been reported. The electrochemical data on aluminum porphyrins with anionic axial ligands are also sparse and to date have been limited to a single report involving (OEP)Al(OH).[5] The present series of measurements on (P)AlCl and (P)Al(R) were carried out in CH_2Cl_2, benzonitrile, and THF. In addition, the molecular structure of methyl(2,3,7,8,12,13,17,18-octaethylporphinato)aluminum(III) was determined by X-ray diffraction and provides the first structural data for an aluminum porphyrin complex.

Experimental Section

Chemicals. Synthesis and handling of each Al(III) porphyrin were carried out under an argon atmosphere. All common solvents were freshly distilled under an inert atmosphere. The (P)AlCl complexes were synthesized by metalation of (OEP)H_2 or (TPP)H_2 with $AlCl_3$ in benzonitrile according to literature methods.[26] Spectroscopic grade methylene chloride was distilled from CaH_2 before use. Reagent grade benzonitrile (PhCN) was distilled over P_2O_5 under vacuum prior to use. HPLC grade tetrahydrofuran (THF) was twice distilled under a nitrogen atmosphere, first from CaH_2 and then from sodium/benzophenone just prior to use. These solvents were purchased from Fisher Scientific Co. Tetrabutylammonium perchlorate (TBAP) and tetrabutylammonium hexafluorophosphate (TBA(PF_6)), purchased from Fluka, were twice recrystallized from absolute ethanol and dried in a vacuum oven at 40 °C prior to use.

General Procedure for Preparation of (P)Al(R). Alkyl- or aryllithium (6 mmol) in ether was added dropwise to (OEP)AlCl or (TPP)AlCl (0.6

(1) (a) Université de Bourgogne (Dijon). (b) Université de Rabat. (c) University of Houston. (d) Université de Nancy I.
(2) Guilard, R.; Kadish, K. M. *Chem. Rev.* **1988**, *88*, 1121.
(3) Guilard, R.; Lecomte, C.; Kadish, K. M. *Struct. Bonding* **1987**, *64*, 205.
(4) Kadish, K. M. *Prog. Inorg. Chem.* **1986**, *34*, 435.
(5) Fuhrhop, J.-H.; Kadish, K. M.; Davis, D. G. *J. Am. Chem. Soc.* **1973**, *95*, 5140.
(6) Kadish, K. M.; Maiya, G. B.; Xu, Q. Y. *Inorg. Chem.* **1989**, *28*, 2518.
(7) Kadish, K. M.; Boisselier-Cocolios, B.; Coutsolelos, A.; Mitaine, P.; Guilard, R. *Inorg. Chem.* **1985**, *24*, 4521.
(8) Coutsolelos, A.; Guilard, R. *J. Organomet. Chem.* **1983**, *253*, 273.
(9) Kadish, K. M.; Cornillon, J.-L.; Cocolios, P.; Tabard, A.; Guilard, R. *Inorg. Chem.* **1985**, *24*, 3645.
(10) Kadish, K. M.; Boisselier-Cocolios, B.; Cocolios, P.; Guilard, R. *Inorg. Chem.* **1985**, *24*, 2139.
(11) Tabard, A.; Guilard, R.; Kadish, K. M. *Inorg. Chem.* **1986**, *25*, 4277.
(12) Cornillon, J.-L.; Anderson, J. E.; Kadish, K. M. *Inorg. Chem.* **1986**, *25*, 2611.
(13) Cornillon, J.-L.; Anderson, J. E.; Kadish, K. M. *Inorg. Chem.* **1986**, *25*, 991.
(14) Hoshino, M.; Hirai, T. *J. Phys. Chem.* **1987**, *91*, 4510.
(15) Hoshino, M.; Yamaji, M.; Hama, Y. *Chem. Phys. Lett.* **1986**, *125*, 369.
(16) Hoshino, M.; Ida, H.; Yasufuku, K.; Tanaka, K. *J. Phys. Chem.* **1986**, *90*, 3984.
(17) Yamaji, M.; Hama, Y.; Arai, S.; Hoshino, M. *Inorg. Chem.* **1987**, *26*, 4375.
(18) Cocolios, P.; Guilard, R.; Bayeul, D.; Lecomte, C. *Inorg. Chem.* **1985**, *24*, 2058.
(19) Cocolios, P.; Guilard, R.; Fournari, P. *J. Organomet. Chem.* **1979**, *179*, 311.
(20) Giraudeau, A.; Louati, A.; Callot, H. J.; Gross, M. *Inorg. Chem.* **1981**, *20*, 769.
(21) Kadish, K. M.; Tabard, A.; Zrineh, A.; Ferhat, M.; Guilard, R. *Inorg. Chem.* **1987**, *26*, 2459.
(22) Takeda, N.; Inoue, S. *Bull. Chem. Soc. Jpn.* **1978**, *51*, 3564.
(23) Inoue, S.; Takeda, N. *Bull. Chem. Soc. Jpn.* **1977**, *50*, 984.
(24) Kuroki, M.; Aida, T.; Inoue, S. *J. Am. Chem. Soc.* **1987**, *109*, 4737.
(25) Murayama, H.; Inoue, S.; Ohkatsu, Y. *Chem. Lett.* **1983**, 381.
(26) Kaizu, Y.; Misu, N.; Tsuji, K.; Kaneko, Y.; Kobayashi, H. *Bull. Chem. Soc. Jpn.* **1985**, *58*, 103.

0020-1669/90/1329-4476$02.50/0

Table I. Reaction Yields and Mass Spectral Data for (P)AlCl and (P)Al(R)

			fragment							
			[(P)Al(R) + H]$^+$		[(P)Al(R)]$^{\cdot+}$		[(P)Al + H]$^{\cdot+}$		[(P)Al]$^+$	
porphyrin, P	ax ligand	yield,[a] %	m/z	% abund	m/z	% abund	m/z	% abund	m/z	% abund
TPP	Cl^-	91	675	100	674	78	640	52	639	55
	CH_3	75	655	2	654	8	640	100	639	90
	n-C_4H_9	29	697	18	696	19	640	96	639	100
	C_6H_5	28	717	3	716	2	640	100	639	76
OEP	Cl^-	94	595	100	594	93	560	1	559	2
	CH_3	67			574	1	560	95	559	100
	n-C_4H_9	46	617	1	616	1	560	89	559	100
	C_6H_5	44	637	5	636	3	560	93	559	100

[a] Reaction yields for (TPP)Al(C_6F_4H) and (OEP)Al(C_6F_4H) are 26 and 28%, respectively.

Table II. Crystallographic Data for (OEP)Al(CH_3)

compd; formula; fw	(OEP)Al(CH_3); $C_{37}H_{47}N_4Al$; 574.79
space group	triclinic, $P\bar{1}$
a–c, Å	10.432 (2), 10.727 (3), 15.959 (5)
α–γ, deg	72.17 (3), 72.93 (3), 82.40 (2)
V, Å^3; Z; ρ_{calcd}, g cm^{-3}	1623.5; 2; 1.18
λ, Å; μ, cm^{-1}	1.54433 (Cu Kα); 6.95
$R(F)$, %; $R_w(F)$, %; GOF	7.11; 8.67; 1.98

Table III. Fractional Coordinates, Standard Deviations, and Equivalent Temperature Factors (Å^2) of Methyl(2,3,7,8,12,13,17,18-octaethylporphinato)aluminum(III)

atom	x	y	z	B
Al	0.41205 (8)	0.50645 (8)	0.26391 (6)	3.94 (2)
N(1)	0.5930 (2)	0.4480 (2)	0.2906 (2)	4.54 (6)
N(2)	0.4674 (2)	0.4058 (3)	0.1689 (2)	4.58 (6)
N(3)	0.2901 (3)	0.6206 (2)	0.1889 (2)	4.66 (6)
N(4)	0.4154 (3)	0.6623 (3)	0.3104 (2)	4.63 (6)
C(1)	0.6732 (3)	0.3423 (3)	0.2729 (3)	5.42 (9)
C(2)	0.7771 (4)	0.3112 (4)	0.3197 (3)	6.2 (1)
C(3)	0.7592 (3)	0.4020 (3)	0.3679 (3)	5.44 (9)
C(4)	0.6443 (3)	0.4826 (3)	0.3500 (2)	4.62 (8)
C(5)	0.5922 (3)	0.5832 (3)	0.3888 (2)	4.70 (8)
C(6)	0.4870 (3)	0.6692 (3)	0.3686 (2)	4.37 (7)
C(7)	0.4411 (4)	0.7782 (3)	0.4057 (2)	5.47 (9)
C(8)	0.3415 (5)	0.8412 (4)	0.3675 (3)	8.7 (1)
C(9)	0.3261 (4)	0.7679 (4)	0.3088 (3)	6.9 (1)
C(10)	0.2357 (5)	0.8018 (4)	0.2568 (3)	8.4 (1)
C(11)	0.2192 (4)	0.7333 (4)	0.2002 (3)	6.4 (1)
C(12)	0.1237 (5)	0.7725 (4)	0.1463 (3)	7.8 (1)
C(13)	0.1348 (4)	0.6788 (4)	0.1028 (3)	6.3 (1)
C(14)	0.2407 (3)	0.5875 (3)	0.1281 (2)	4.96 (8)
C(15)	0.2912 (3)	0.4845 (3)	0.0909 (2)	5.19 (8)
C(16)	0.3981 (3)	0.4012 (3)	0.1089 (2)	4.90 (8)
C(17)	0.4526 (4)	0.2982 (4)	0.0662 (2)	5.53 (9)
C(18)	0.5541 (4)	0.2369 (4)	0.1026 (3)	5.71 (9)
C(19)	0.5636 (3)	0.3051 (3)	0.1654 (2)	5.38 (9)
C(20)	0.6581 (4)	0.2748 (4)	0.2149 (3)	6.2 (1)
C(21)	0.8804 (4)	0.2002 (5)	0.3170 (3)	7.3 (1)
C(22)	0.9967 (5)	0.2317 (6)	0.2359 (4)	9.6 (2)
C(23)	0.8425 (4)	0.4182 (4)	0.4254 (3)	6.8 (1)
C(24)	0.9313 (5)	0.5325 (6)	0.3788 (4)	8.8 (2)
C(25)	0.4992 (4)	0.8149 (4)	0.4699 (3)	6.2 (1)
C(26)	0.6250 (5)	0.8921 (5)	0.4221 (3)	7.8 (1)
C(27)[a]	0.234 (1)	0.9390 (9)	0.4037 (8)	6.3 (3)
C(28)[a]	0.278 (1)	1.072 (1)	0.3329 (9)	9.4 (4)
C(271)[a]	0.299 (1)	0.992 (1)	0.3527 (8)	6.5 (3)
C(281)[a]	0.162 (1)	0.983 (1)	0.4205 (7)	9.3 (4)
C(29)	0.0384 (6)	0.8997 (6)	0.1362 (4)	9.8 (2)
C(30)	−0.0766 (7)	0.8783 (7)	0.2118 (6)	12.0 (3)
C(31)	0.0548 (5)	0.6718 (4)	0.0408 (3)	8.4 (1)
C(32)	−0.0674 (7)	0.5918 (6)	0.0901 (5)	11.6 (2)
C(33)	0.4022 (4)	0.2675 (4)	−0.0045 (3)	6.6 (1)
C(34)	0.2912 (5)	0.1734 (5)	0.0391 (3)	8.0 (1)
C(35)	0.6406 (4)	0.1204 (4)	0.0839 (3)	7.3 (1)
C(36)	0.5877 (6)	−0.0089 (5)	0.1530 (4)	9.3 (2)
C(41)	0.2894 (3)	0.3902 (4)	0.3649 (2)	5.57 (9)

[a] The site occupations of C(27) and C(28) were constrained to be equal, and the site occupation factors of C(271) and C(281) were constrained to m[C(28)] + m[C(281)] = 1. The refined values are 0.50 (2).

Table IV. Main Bond Distances (Å), Angles (deg), and Standard Deviations in the Coordination Polyhedron

	Bond Distances		
Al–N(1)	2.033 (3)	Al–N(4)	2.030 (3)
Al–N(2)	2.034 (3)	Al–C(41)	1.942 (3)
Al–N(3)	2.033 (3)		
	Bond Angles		
N(1)–Al–N(2)	86.7 (1)	N(1)–Al–C(41)	103.0 (1)
N(1)–Al–N(4)	87.4 (1)	N(2)–Al–C(41)	103.8 (1)
N(2)–Al–N(3)	87.0 (1)	N(3)–Al–C(41)	103.4 (1)
N(3)–Al–N(4)	86.9 (1)	N(4)–Al–C(41)	102.6 (2)

mmol) in toluene (200 cm^3) as the progress of the reaction was monitored by UV–visible spectroscopy. The reaction mixture was purified by chromatography over a silica gel column (height 3 cm, diameter 3 cm) to eliminate the remaining organolithium reactant, which was in excess. Toluene was used as the mobile phase in this separation. The organic solution was taken to dryness under reduced pressure and the crude product then washed with heptane and dried. Yields for the eight σ-bonded complexes synthesized by this method are given in Table I.

Instrumentation. Mass spectra were recorded in the electron-impact mode with a Finnigan 3300 spectrometer: ionizing energy 30–70 eV, ionizing current 0.4 mA, and source temperature 250–400 °C. ^{1}H NMR spectra were obtained at 400 MHz by using a Bruker WM 400 spectrometer of the Cerema ("Centre de Résonance Magnétique de l'Université de Bourgogne"). Each solution contained between 3 and 5 mg of the complex in a deuterated solvent. Infrared spectra were recorded on a Perkin-Elmer 580B infrared spectrometer. Samples were prepared as 1% dispersions in a CsI pellet. UV–visible spectra were recorded on a Perkin-Elmer 559 spectrometer or an IBM Model 9430 spectrometer.

Cyclic voltammograms were obtained with a PAR Model 174A polarographic analyzer or an IBM Model EC 225 voltammetric analyzer using a three-electrode system. The working electrode was a platinum disk with surface area of ca. 0.8 mm^2. A homemade saturated calomel electrode (SCE) was used as the reference electrode and was separated from the bulk solution by a fritted-glass bridge. The auxiliary electrode was a platinum wire with a large surface area. High-purity nitrogen or argon was used to deaerate the solution as well as to maintain an inert-gas atmosphere above the solution during the experiments. All experiments were carried out in the dark due to the high light sensitivity of the σ-bonded complexes.[22-25]

Crystal and Molecular Structure Determination. A suitable crystal of (OEP)Al(CH_3) was obtained by recrystallization from a toluene/heptane mixture. Preliminary Weissenberg photographs revealed a triclinic cell (see Table II). A total of 6129 reflections were collected at room temperature with monochromatized Cu Kα radiation; 4359 reflections ($I > 3\sigma(I)$) were used to determine the crystal structure. The data were reduced with the SDP program.[27] The structure was solved by interpretation of the Patterson map and by subsequent Fourier syntheses. It was refined via standard least-squares techniques (SHELX 76).[28] Scattering factors were taken from refs 28 and 29. At the end of the non-hydrogen atom refinements, difference Fourier maps revealed one disordered ethyl group (C(27) and C(28)). This problem was solved by refining two different ethyl positions (C(271), C(281), C(27), C(28)). All hydrogen atoms except those linked to the disordered ethyl group

(27) SDP: Structure Determination Package; Enraf-Nonius: Delft, The Netherlands, 1977.
(28) Sheldrick, G. M. *SHELX 76: Program of Crystal Structure Determination*; University of Göttingen: Göttingen, FRG, 1976.
(29) *International Tables for X-ray Crystallography*, Kynoch: Birmingham, U.K., 1974; Vol. IV.

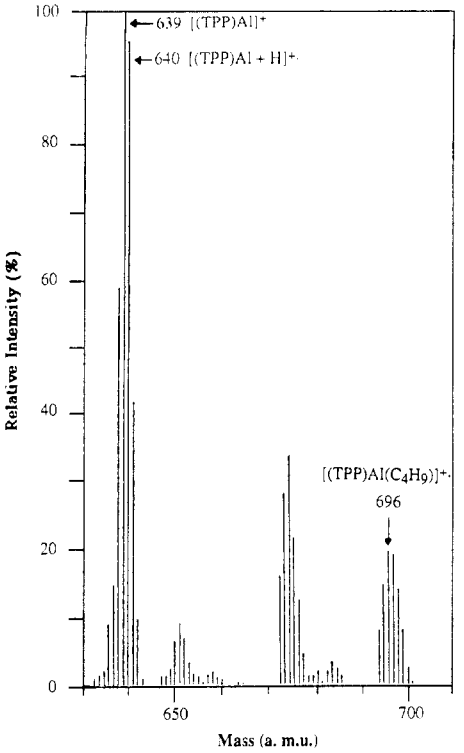

Figure 1. Mass spectrum of (TPP)Al(n-C_4H_9).

Table V. Solid-State IR Data (ν, cm^{-1}) for (P)AlCl and (P)Al(R) (CsI Pellets)

porphyrin, P	ax ligand	ν_{Al-C}	ν_{Al-Cl}
TPP	Cl^-		463
	CH_3	626	
	n-C_4H_9	457	
	C_6H_5	423	
	C_6F_4H	417	
OEP	Cl^-		448
	CH_3	611	
	n-C_4H_9	435	
	C_6H_5	422	
	C_6F_4H	416	

were found in the difference Fourier synthesis and were included as fixed contributors to the least-squares process. A summary of the least-squares results is given in Table II. Fractional coordinates of the non-hydrogen atoms are given in Table III. The main bond distances and angles are given in Table IV. Other bond distances and angles, anisotropic thermal parameters, hydrogen coordinates, least-squares planes, structure factors, and experimental conditions are given as supplementary material.

Results and Discussion

Spectroscopic Characterization. The mass spectrum of (TPP)Al(C_4H_9) is illustrated in Figure 1, and a summary of mass spectral data for each investigated derivative is given in Table I. The data in this table are in excellent agreement with the molecular formulas (P)Al(R) or (P)AlCl. Between two and four major fragments are observed for each (P)Al(R) complex. These are $[(P)Al(R) + H]^+$, $[(P)Al(R)]^{\bullet+}$, $[(P)Al + H]^{\bullet+}$, and $[(P)Al]^+$. The small relative intensities of the molecular peak for (TPP)Al(R) (2–19%) and (OEP)Al(R) (1–3%) are consistent with a facile cleavage of the σ-bonded alkyl or aryl ligand.[8,19] These data also indicate that the aluminum–carbon bond in (P)Al(R) is less stable than the corresponding metal–carbon bond in (P)Ga(R),[7,8] (P)In(R),[10,11,19] or (P)Tl(R),[21] all of which have molecular peaks of significantly larger intensity.

Infrared data of the 10 investigated (P)AlCl and (P)Al(R) complexes are given in Table V, and an IR spectrum of (OEP)Al(CH_3) is represented in Figure 2. The Al–Cl vibrations are located at 463 cm^{-1} for (TPP)AlCl and 448 cm^{-1} for (OEP)AlCl, while the (TPP)Al(R) and (OEP)Al(R) derivatives show Al–C vibrations in the range 416–626 cm^{-1}. Both sets of values are in good agreement with vibrational modes for non-porphyrin complexes containing Al–Cl or Al–C bonds.[30–32]

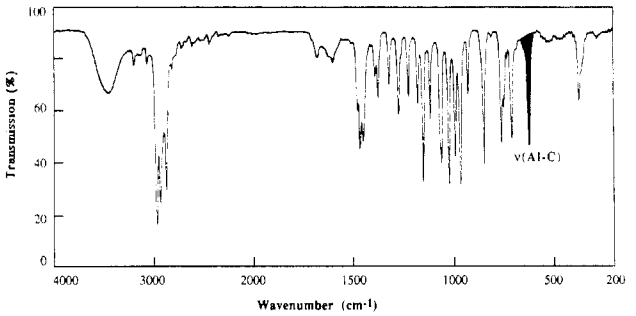

Figure 2. IR spectrum of (OEP)Al(CH_3)(CsI Pellet).

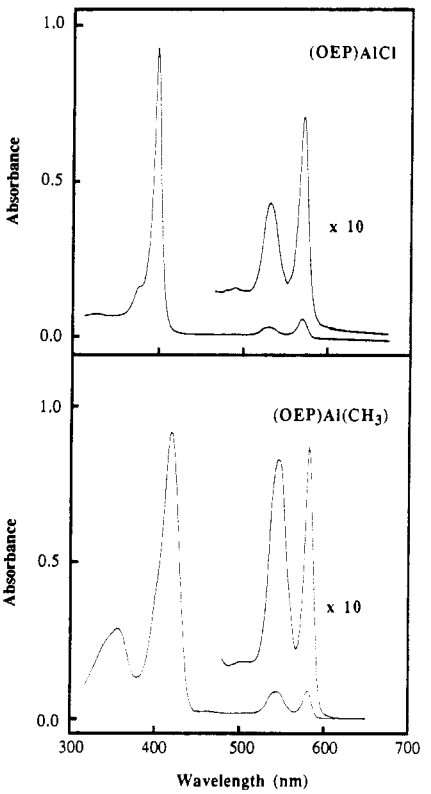

Figure 3. Electronic absorption spectra of (OEP)AlCl and (OEP)Al(CH_3) in C_6H_6.

The UV–visible spectral data for (P)AlCl and (P)Al(R) in benzene are summarized in Table VI, and examples of UV–visible spectra for (OEP)AlCl and (OEP)Al(CH_3) are shown in Figure 3. The (P)AlCl complexes have a single Soret band at 418 nm (P = TPP) or 399 nm (P = OEP) and can be characterized as normal metalloporphyrin spectra.[33] This contrasts with the (P)Al(R) derivatives, which have a split Soret band and are characterized as having hyperporphyrin spectra.[33] The split Soret bands of (P)Al(R) are labeled as bands I and II in Table VI. Band II (the Soret band) occurs between 407 and 436 nm and involves a $\pi \rightarrow \pi^*$ porphyrin electronic transition. It is red shifted by 4–24 nm compared to the corresponding transitions of (P)AlCl. Band I of (P)Al(R) occurs between 320 and 376 nm and involves a transition from the metal to the macrocycle ($a_{2u}(3p_z)_{metal} \rightarrow e_g(\pi^*)_{porphyrin}$). This band is not present in either (OEP)AlCl or (TPP)AlCl.

(30) Goedken, V. L.; Ito, H.; Ito, T. *J. Chem. Soc., Chem. Commun.* **1984**, 1453.
(31) Jennings, J. R.; Lloyd, J. E.; Wade, K. *J. Chem. Soc.* **1965**, 5083.
(32) Breakell, K. R.; Rendle, D. F.; Storr, A.; Trotter, J. *J. Chem. Soc., Dalton Trans.* **1975**, 1584.
(33) Gouterman, M. In *The Porphyrins*; Dolphin, D., Ed.; Academic: New York, 1978; Vol. III, Chapter I.

Table VI. UV–Visible Data for (P)AlCl and (P)Al(R) Complexes in Benzene (λ, nm; ε, M^{-1} cm^{-1})

		λ_{max} ($10^{-3}\epsilon$)					
		Soret region		visible region			
porphyrin, P	ax ligand	band I[a]	band II[b]	Q(2,0)	Q(1,0)	Q(0,0)	ε(II)/ε(I)
TPP	Cl^-		418 (115.5)	506 (0.1)	550 (7.0)	587 (1.7)	
	CH_3	340 (20.3)	433 (251.5)	520 (0.1)	563 (12.0)	605 (5.2)	12.40
	n-C_4H_9	376 (11.6)	436 (34.4)	516 (0.5)	567 (2.1)	614 (1.8)	2.97
	C_6H_5	340 (34.4)	432 (445.3)	520 (0.1)	562 (16.2)	603 (4.9)	12.95
	C_6F_4H	320 (5.3)	422 (208.7)	512 (0.1)	552 (7.8)	592 (1.2)	39.70
OEP	Cl^-		399 (244.6)	493 (0.3)	532 (8.2)	572 (16.5)	
	CH_3	356 (25.2)	419 (106.2)	504 (0.1)	548 (9.8)	582 (11.1)	4.22
	n-C_4H_9	366 (43.7)	423 (52.7)	512 (0.1)	547 (8.1)	586 (5.5)	1.21
	C_6H_5	356 (26.6)	419 (115.8)	503 (0.1)	548 (13.1)	582 (11.8)	4.35
	C_6F_4H	334 (10.9)	407 (299.3)	494 (0.1)	538 (11.4)	578 (18.8)	27.40

[a] Extra absorption band. [b] Soret band, B(0,0).

Table VII. ^1H NMR Data for (P)AlCl and (P)Al(R) Complexes[a]

				protons of R^1			protons of R^2			protons of R		
porphyrin, P	ax ligand	R^1	R^2	assgnt	multi/intens	δ	assgnt	multi/intens	δ	assgnt	multi/intens	δ
TPP	Cl^-	C_6H_5	H	*o*-H	d/8	+7.98	pyrr H	s/8	+9.08			
				m-H, *p*-H	m/12	+7.42						
	CH_3	C_6H_5	H	*o*-H	d/8	+8.04	pyrr H	s/8	+9.10	CH_3	s/3	−6.03
				m-H, *p*-H	m/12	+7.42						
	n-C_4H_9	C_6H_5	H	*o*-H	d/8	+8.10	pyrr H	s/8	+9.11	δ-CH_3	t/3	−0.37
				m-H, *p*-H	m/12	+7.44				γ-CH_2	m/2	−1.06
										β-CH_2	m/2	−2.89
										α-CH_2	t/2	−5.63
	C_6H_5	C_6H_5	H	*o*-H	d/8	+8.07	pyrr H	s/8	+9.07	*o*-H	d/2	+2.48
				m-H, *p*-H	m/12	+7.46				*m*-H	t/2	+5.58
										p-H	t/1	+5.84
	C_6F_4H	C_6H_5	H	*o*-H	d/8	+8.05	pyrr H	s/8	+9.08	*p*-H	m/1	+4.99
				m-H, *p*-H	m/12	+7.43						
OEP	Cl^-	H	C_2H_5	*meso*-H	s/4	+10.39	β-CH_3	t/24	+1.81			
							α-CH_2	m/8	+3.90			
							α′-CH_2	m/8	+4.00			
	CH_3	H	C_2H_5	*meso*-H	s/4	+10.40	β-CH_3	t/24	+1.85	CH_3	s/3	−6.48
							α-CH_2	m/8	+3.94			
							α′-CH_2	m/8	+4.06			
	n-C_4H_9	H	C_2H_5	*meso*-H	s/4	+10.39	β-CH_3	t/24	+1.84	δ-CH_3	t/3	−0.62
							α-CH_2	m/8	+3.94	γ-CH_2	m/2	−1.86
							α′-CH_2	m/8	+4.05	β-CH_2	m/2	−3.33
										α-CH_2	t/2	−6.10
	C_6H_5	H	C_2H_5	*meso*-H	s/4	+10.41	β-CH_3	t/24	+1.85	*o*-H	d/2	+2.18
							α-CH_2	m/8	+3.99	*m*-H	t/2	+5.26
							α′-CH_2	m/8	+4.06	*p*-H	t/1	+5.50
	C_6F_4H	H	C_2H_5	*meso*-H	s/4	+10.41	β-CH_3	t/24	+1.85	*p*-H	m/1	+4.65
							α-CH_2	m/8	+3.99			
							α′-CH_2	m/8	+4.13			

[a] Spectra were recorded in C_6D_6 at 21 °C with $SiMe_4$ as internal reference; chemical shifts (δ, ppm) downfield from $SiMe_4$ are defined as positive. Key: R^1 = porphyrin methine group; R^2 = porphyrin pyrrole group; R = axial ligand; s = singlet; d = doublet; t = triplet; m = multiplet.

The ratio of molar absorptivity between band II and band I of a given complex, ε(II)/ε(I), is related to the electron-donating ability of the σ-bonded axial ligand. Values of ε(II)/ε(I) for (P)Al(R) are listed in Table VI and range between 2.97 and 39.70 (TPP derivatives) or between 1.21 and 27.40 (OEP derivatives). The two porphyrins with the strongest electron-donating σ-bonded group (n-C_4H_9) have the smallest ratio of molar absorptivities, while those with the weakest electron-donating group (C_6F_4H) have the highest ratio. Also, the ratio of ε(II)/ε(I) is smaller for derivatives in the OEP series than for those in the TPP series, and this agrees with the higher basicity of the OEP porphyrin macrocycle.

The UV–visible data for (P)Al(R) are comparable to data obtained for the analogous σ-bonded (P)M(R) porphyrins with gallium,[7] indium,[10] or thallium[21] central metals. However, the band I molar absorptivity is generally larger for (P)Al(R) than for the other group 13 σ-bonded complexes with the same porphyrin ring, P.

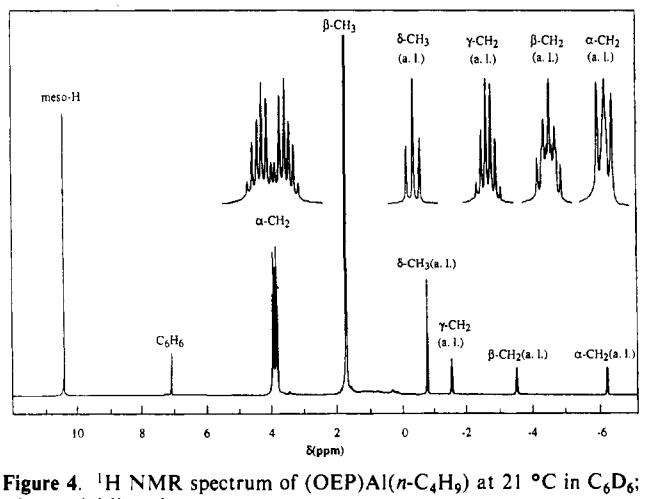

Figure 4. ^1H NMR spectrum of (OEP)Al(n-C_4H_9) at 21 °C in C_6D_6; a.l. = axial ligand.

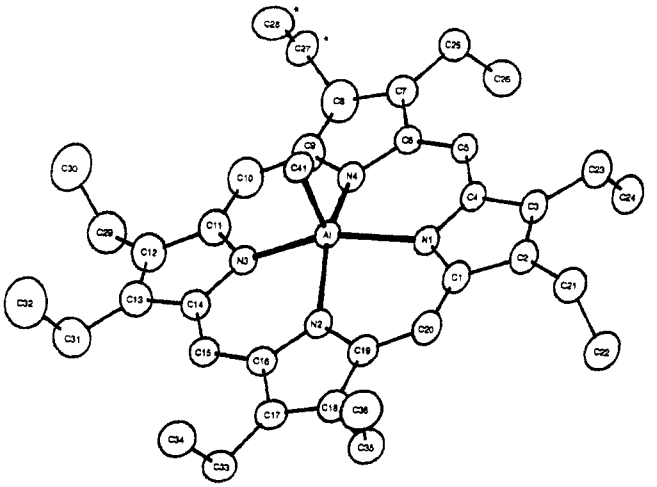

Figure 5. ORTEP diagram of (OEP)Al(CH_3) with numbering scheme utilized.

A characteristic ^1H NMR spectrum of the σ-bonded derivatives is given in Figure 4 for (OEP)Al(C_4H_9), while data for each (P)AlCl or (P)Al(R) complex are summarized in Table VII. Meso proton NMR signals of octaethylporphyrins with trivalent central metals are generally located in the range 10.13–10.39 ppm, and the data in Table VII thus support the assignment of trivalent aluminum(III). Methylene protons of OEP ethyl groups give two multiplets at around 4.00 ppm and are typical of an ABX_3 coupling due to the inequivalence of the two methylene protons. An ABX_3 coupling was also observed for (P)M(R), where M = Ga(III),[7,8] In(III),[11,19] or Tl(III).[21]

The similarity in meso proton chemical shifts of the four σ-bonded metalloporphyrins and (OEP)AlCl indicates that the macrocycle proton chemical shifts are independent of the electron-donating properties of the bound axial ligand. This is also the case for (OEP)Ga(R)[7,8] but not for (OEP)In(R)[10,11,19] or (OEP)Tl(R)[21] under similar solution conditions.

The pyrrole proton signals of (TPP)AlCl and (TPP)Al(R) are in the range 9.07–9.11 ppm and show no significant dependence upon the electronic character of the axial ligand. The phenyl meta and para proton resonances of these complexes appear as a multiplet between 7.42 and 7.46 ppm, while the ortho proton signals appear as a doublet between 7.98 and 8.10 ppm. These data indicate that the ortho and meta protons are equivalent and that there is a free rotation of the phenyl groups around the C_{meso}–C_{phenyl} bond.

A coordination of the alkyl or aryl group to the Al(III) center of (P)Al(R) is indicated by the fact that the shielding of the axial ligand protons is dependent upon the ring current of the porphyrin macrocycle. A similar behavior has been reported for gallium,[8] indium,[11,19] and thallium[21] σ-bonded porphyrins.

Molecular Structure of Methyl(2,3,7,8,12,13,17,18-octaethylporphinato)aluminum(III). Figure 5 gives a representation of (OEP)Al(CH_3) with the numbering scheme used. The aluminum atom is pentacoordinated by the four nitrogen atoms of the macrocycle and the carbon of the σ-bonded methyl ligand. The resulting coordination polyhedron is a square pyramid of C_{4v} symmetry. The four Al–N distances, as well as the N–Al–CH_3 angles, are statistically equal (⟨Al–N⟩ = 2.033 (3) Å, ⟨N–Al–CH_3⟩ = 103.2 (5)°). The Al–CH_3 bond distance (1.942 (3) Å) is also equal to the Al–CH_3 distance of 1.94 (1) Å in $KAlCl_3(CH_3)$.[34] Of previously synthesized group 13 σ-bonded porphyrins, only crystal structures of (TPP)In(CH_3)[35] and (TPP)Tl(CH_3)[36] have been reported.

Table VIII. Main Characteristics of Five-Coordinated σ-Bonded Metalloporphyrins

compd	⟨M–N⟩, Å	M–C, Å	Δ(4N), Å[a]	ref
(OEP)Al(CH_3)	2.033 (3)	1.942 (3)	0.47	this work
(TPP)In(CH_3)	2.205 (10)	2.132 (15)	0.78	35
(TPP)Tl(CH_3)	2.291 (10)	2.147 (12)	0.98	36
(TPP)Fe(C_6H_5)	1.963 (11)	1.955 (3)	0.175	37
(OEP)Rh(CH_3)	2.031 (10)	2.031 (6)	0.05	38

[a] Δ(4N): distance of the metal from the plane of the four nitrogens.

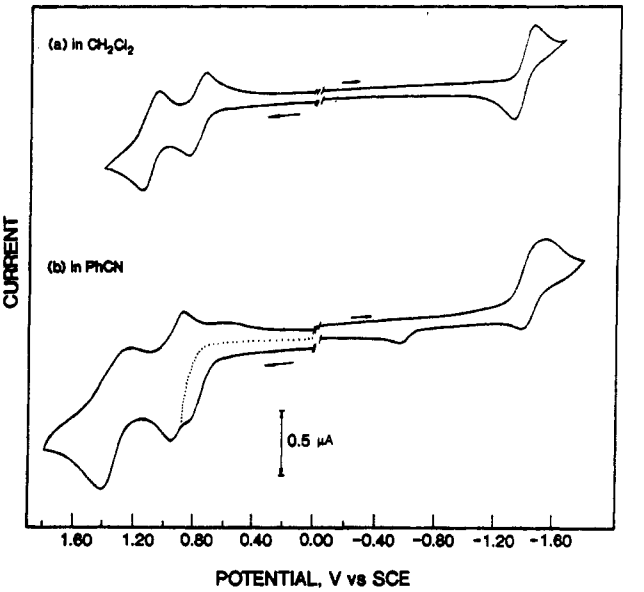

Figure 6. Cyclic voltammograms showing the oxidation of (OEP)AlCl in (a) CH_2Cl_2, 0.1 M TBAP and (b) PhCN, 0.1 M TBA(PF_6). Scan rate = 0.1 V s^{-1}.

Table VIII summarizes several bonding characteristics of (OEP)Al(CH_3) and also gives data for (TPP)Fe(C_6H_5)[37] and (TPP)M(CH_3), where M = In,[35] Tl,[36] or Rh.[38] As expected, stereochemical parameters of the group 13 σ-bonded porphyrins are directly linked to the size of the metal atom, i.e. the larger the metal atom, the larger the metal–ligand distance. Also the structures of group 13 compounds differ from those of the transition-metal complexes.[3]

Electrode Reactions of (OEP)AlCl and (TPP)AlCl. (OEP)AlCl undergoes two reversible oxidations and a single reversible reduction in CH_2Cl_2, 0.1 M TBAP. These reactions occur at $E_{1/2}$ = +0.79, +1.11, and −1.38 V, as shown by the cyclic voltammogram in Figure 6a. The absolute potential difference between the two oxidations in CH_2Cl_2 is 0.32 V, thus suggesting that both reactions are porphyrin ring centered.[2-5] In addition, the 2.17-V difference in $E_{1/2}$ between the first oxidation and the first reduction of (OEP)AlCl agrees with the $\Delta E_{1/2}$ = 2.25 ± 0.15 V generally obtained for formation of porphyrin π cation and π anion radicals.[5]

The shape of the voltammogram for reduction of (OEP)AlCl varies significantly as a function of the solvent system. A well-defined reversible one-electron reduction occurs in CH_2Cl_2, but two overlapping reduction peaks are obtained in PhCN (see Figure 6b). On the other hand, as the temperature is lowered from 23 to −10 °C, the first reduction in PhCN becomes more reversible. This suggests that the overall electron transfer involves a chemical reaction that occurs either before or after the one-electron reduction of (OEP)AlCl. This chemical reaction may involve a dissociation of Cl^-, but this was not investigated as part of the present study.

(OEP)AlCl undergoes three, rather than two, oxidations in PhCN containing 0.1 M TBA(PF_6) (see Figure 6b). These reactions occur at E_p = 0.82 V, $E_{1/2}$ = 0.92 V, and $E_{1/2}$ = 1.33 V.

(34) Atwood, J. L.; Heneir, D. C.; Newberry, W. R. *Cryst. Struct. Commun.* **1974**, *3*, 615.
(35) Lecomte, C.; Protas, J.; Cocolios, P.; Guilard, R. *Acta Crystallogr., Sect. B* **1980**, *B36*, 2769.
(36) Henrick, K.; Matthews, R. W.; Tasker, P. A. *Inorg. Chem.* **1977**, *16*, 3293.
(37) Doppelt, P. *Inorg. Chem.* **1984**, *23*, 4009.
(38) Takeda, A.; Syal, S. K.; Sasada, Y.; Omura, T.; Ogoshi, H.; Yoshida, Z. I. *Acta Crystallogr., Sect. B* **1976**, *B32*, 62.

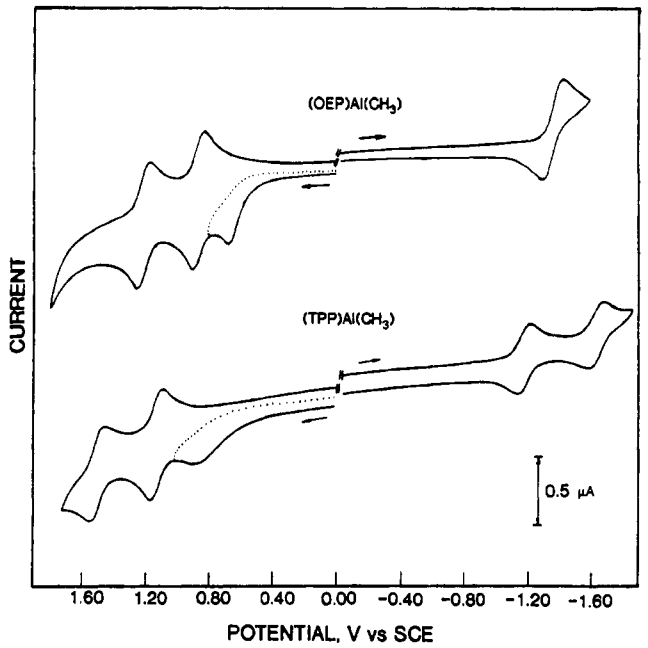

Figure 7. Cyclic voltammograms of (OEP)Al(CH_3) and (TPP)Al(CH_3) in PhCN, 0.1 M TBA(PF_6). Scan rate = 0.1 V s^{-1}.

The first is irreversible, while the second and the third are reversible. The same complex undergoes two oxidations in THF, 0.1 M TBA(PF_6). These electrode reactions occur at E_p = 0.96 V and $E_{1/2}$ = 1.07 V. The positive potential limit of THF is less than the limit of either PhCN or CH_2Cl_2, and this prohibits the monitoring of a third electrochemical process in this solvent at more positive potentials.

The second and the third oxidations of (OEP)AlCl in PhCN have $E_{1/2}$ values that are similar to the second and third oxidations of (OEP)Al(R) in the same solvent media. In the case of (OEP)Al(R), these reactions have been characterized as due to a non-σ-bonded complex that is generated after cleavage of the Al–C bond (see following sections). This suggests that the first oxidation of (OEP)AlCl involves the Cl^- counterion and that the latter two reactions at more positive potentials involve a stepwise one-electron oxidation of electrogenerated $[(OEP)Al]^+$ and $[(OEP)Al]^{2+}$. A dissociation of the Cl^- counterion is known to occur in bonding solvents, and the oxidation of Cl^- from (OEP)Ge(C_6H_5)Cl has been reported to occur at E_p = 1.10 V in PhCN.[39]

(TPP)AlCl undergoes two reversible reductions at $E_{1/2}$ = −1.10 and −1.45 V in CH_2Cl_2 0.1 M TBAP. The absolute potential difference between these two processes is 0.35 V, which suggests that both electron additions occur at the porphyrin π-ring system to generate an anion radical and dianion.[4] The singly reduced product is unstable in both PhCN and THF, and this results in a lack of reversibility that may be associated with some decomposition of the complex. A dissociation of the Cl^- counterion may occur after electroreduction of (TPP)AlCl, but this was also not investigated in the present study, which concentrated mainly on the σ-bonded derivatives.

The electrooxidation of (TPP)AlCl is also complicated in CH_2Cl_2, THF, and PhCN. In CH_2Cl_2, 0.1 M TBAP, there are three reversible oxidations located at $E_{1/2}$ = 0.92, 1.16, and 1.43 V. The first involves a two-electron-transfer step, while the second and third each involve a single electron transfer. The apparent two-electron oxidation peak may be due to an equilibrium between the original complex and the anion of the supporting electrolyte, to oxidation of Cl^- and/or to oxidation of one or more porphyrin decomposition products. This was not investigated in detail, but it should be noted that a μ-oxo dimer of the type $[(TPP)Al]_2O$ is known[40] and such a species might conceivably be formed as a side product upon electrooxidation of (TPP)AlCl.

Table IX. Half-Wave[a] or Peak Potentials (V vs SCE) for Oxidation–Reduction of (OEP)Al(R) and (TPP)Al(R) Complexes, Where R = CH_3, n-C_4H_9, or C_6H_5

		ax ligand of OEP complexes			ax ligand of TPP complexes		
solvent	electrode reacn	CH_3	C_4H_9	C_6H_5	CH_3	C_4H_9	C_6H_5
PhCN[d]	1st redn	−1.45	−1.48	−1.47	−1.18	−1.19	−1.18
	2nd redn				−1.63	−1.64	−1.60
	1st oxidn[b]	0.71	0.73	0.76	0.88	0.82	0.80
	2nd oxidn[c]	0.91	0.91	0.91	1.12	1.13	1.12
	3rd oxidn[c]	1.35	1.36	1.35	1.50	1.52	1.48
THF[d]	1st redn	−1.34	−1.41	−1.33	−1.15	−1.08	−0.94
	2nd redn				−1.58	−1.40	−1.40
	1st oxidn[b]	0.55	0.68	0.65	0.64	0.59	0.78
	2nd oxidn[c]	1.05	1.11	1.04	1.25	1.19	1.05
CH_2Cl_2[e]	1st redn	−1.49	−1.50	−1.44	−1.21	−1.16	−1.20
	2nd redn				−1.60	−1.52	−1.55
	1st oxidn[b]	0.75	0.61	0.75	0.88	0.70	0.78
	2nd oxidn[c]	0.83	0.83	0.88	0.97	1.03	0.93
	3rd oxidn[c]	1.16	1.17	1.27	1.21	1.20	1.17

[a] All listed potentials are $E_{1/2}$ values unless otherwise noted. [b] Irreversible oxidation due to cleavage of the Al–C bond in electrogenerated $[(P)M(R)]^+$. [c] Values of $E_{1/2}$ correspond to potentials for oxidation of electrogenerated $[(P)Al]^+$ and $[(P)Al]^{2+}$. [d] Supporting electrolyte is 0.1 M TBA(PF_6). [e] Supporting electrolyte is 0.1 M TBAP.

Electrode Reactions of (OEP)Al(R) and (TPP)Al(R). The electrochemistry of (OEP)Al(R) and (TPP)Al(R), where R = CH_3, C_4H_9, or C_6H_5, was investigated in PhCN, THF, and CH_2Cl_2 containing either 0.1 M TBAP or 0.1 M TBA(PF_6) as supporting electrolyte. The best voltammetric behavior is obtained in PhCN containing 0.1 M TBA(PF_6), and cyclic voltammograms for the oxidation and reduction of (OEP)Al(CH_3) and (TPP)Al(CH_3) under these solution conditions are shown in Figure 7.

Half-wave or peak potentials for each electrode reaction of (P)Al(R) in PhCN, THF, and CH_2Cl_2 are listed in Table IX. The (OEP)Al(R) complexes undergo a single one-electron reduction, while (TPP)Al(R) is reduced via two one-electron-transfer steps. All three reactions are reversible in PhCN, 0.1 M TBA(PF_6) and occur at potentials that vary only slightly with changes in the σ-bonded axial ligand. For example, the one-electron reduction of (OEP)Al(R) in PhCN occurs at $E_{1/2}$ values between −1.45 and −1.48 V for complexes for R = CH_3, C_4H_9, or C_6H_5.

There is also only a small shift of $E_{1/2}$ for reduction of the three (TPP)Al(R) complexes in PhCN ($E_{1/2}$ ranges from −1.18 to −1.19 V for the first reduction and from −1.60 to −1.64 V for the second reduction). These values are similar to half-wave potentials for reduction of other group 13 (P)M(R) complexes in PhCN and fall within the range of values expected for formation of π anion radicals and dianions as shown by eqs 1 and 2.

$$(P)M(R) + e \rightleftarrows [(P)M(R)]^{\bullet-} \quad (1)$$

$$[(P)M(R)]^{\bullet-} + e \rightleftarrows [(P)M(R)]^{2-} \quad (2)$$

The absolute half-wave potential difference between the first and the second reductions of a given (TPP)Al(R) complex ranges between 0.42 and 0.45 V in PhCN, between 0.35 and 0.39 V in CH_2Cl_2, and between 0.32 and 0.46 V in THF. All three values are in good agreement with the 0.42 ± 0.05 V separation generally observed for porphyrin π-ring-centered reductions.[2-5]

The oxidation potentials and overall electrochemical behavior of a given (P)Al(R) complex depend upon the specific solvent/supporting electrolyte system. Solutions with TBAP as supporting electrolyte give better defined voltammograms than those with TBA(PF_6) for investigating the oxidations of (OEP)Al(R) and (TPP)Al(R) in CH_2Cl_2. Under these solution conditions, both the OEP and TPP σ-bonded derivatives undergo three oxidations.

(39) Kadish, K. M.; Xu, Q. Y.; Barbe, J.-M.; Anderson, J. E.; Wang, E.; Guilard, R. *J. Am. Chem. Soc.* **1987**, *109*, 7705.

(40) Harriman, A.; Osborn, A. D. *J. Chem. Soc., Faraday Trans. 1*, **1983**, *79*, 765.

Table X. Summary of Half-Wave and Peak Potentials (V vs SCE) for the Oxidation–Reduction of (P)M(CH_3) in PhCN, 0.1 M TBA(PF_6)

porphyrin ring	central metal	oxidn			redn	
		E_p[a]	$E_{1/2}$[b]	$E_{1/2}$[b]	$E_{1/2}$	$E_{1/2}$
OEP	Al	0.71	0.91	1.35	−1.45	
	Ga	0.76	1.02	1.44	−1.50	
	In	0.84	1.16	1.47	−1.40	
	Tl		0.74	1.04	−1.38	
TPP	Al	0.88	1.12	1.50	−1.18	−1.63
	Ga	0.88	1.17	1.52	−1.12	−1.55
	In	0.85	1.22	1.55	−1.10	−1.51
	Tl		0.81	1.22	−1.13	−1.51

[a] Irreversible reaction due to resulting cleavage of the metal–carbon bond of electrogenerated $[(P)M(R)]^+$. E_p is given for a scan rate of 0.1 V s^{-1}. [b] Values of $E_{1/2}$ for the Al, Ga, and In complexes are those for electrogenerated $[(P)M]^+$. The values of $E_{1/2}$ for the Tl derivatives correspond to reactions of stable (P)Tl(CH_3) and $[(P)Tl(CH_3)]^{\bullet+}$ species.

Three oxidations are also observed in PhCN containing 0.1 M TBA(PF_6). The first is irreversible, while the second and the third are reversible, as illustrated in Figure 7 for the case of (OEP)Al(CH_3) and (TPP)Al(CH_3).

The data in Table IX are self-consistent and indicate the occurrence of a chemical reaction following the first one-electron oxidation of (P)Al(R) in all three solvents. This reaction involves a cleavage of the σ-bonded R group and leads to formation of $[(P)Al]^+$, as shown by eq 3.

$$(P)Al(R) \rightleftharpoons [(P)Al(R)]^{\bullet+} \rightarrow [(P)Al]^+ + R^{\bullet} \qquad (3)$$

The second and the third oxidations of (OEP)Al(R) and (TPP)Al(R) vary only slightly with changes in the σ-bonded axial ligand and are assigned as involving electrogenerated $[(P)Al]^+$ or $[(P)Al]^{2+}$, as shown in eqs 4 and 5.

$$[(P)Al]^+ \rightleftharpoons [(P)Al]^{2+} + e \qquad (4)$$

$$[(P)Al]^{2+} \rightleftharpoons [(P)Al]^{3+} + e \qquad (5)$$

An $E_{1/2}$ of 0.91 V is obtained for the second oxidation of all three (OEP)Al(R) species in PhCN (eq 4), while $E_{1/2}$ for the third oxidation of the three investigated complexes in the same solvent (eq 5) is either 1.35 or 1.36 V (see Table IX). THF has a less positive potential limit than PhCN, and only two oxidations can be observed in this solvent.

A comparison of cyclic voltammograms for oxidation and reduction of (TPP)M(CH_3), where M = Al, Ga, In, or Tl, is given in Figure 8 and Table X. Exact details as to the electrooxidation and electroreduction mechanisms of (P)Ga(R),[7] (P)In(R),[10,11] and (P)Tl(R)[21] have been reported in the literature, and several comparisons between these three σ-bonded group 13 complexes have already been published.[2-4] However, a comparison of these data with those for (P)Al(R) was not previously possible due to the fact that only two different Al(III) σ-bonded complexes had been synthesized at that time and neither of these had been electrochemically investigated.

As seen in Figure 8, current–voltage curves for reduction of the four (P)M(CH_3) complexes are almost identical in PhCN. This is also the case for electrooxidation of (TPP)Al(CH_3), (TPP)Ga(CH_3), and (TPP)In(CH_3) but not for (TPP)Tl(CH_3). This is consistent with the occurrence of similar oxidation mechanisms for the Al, Ga, and In σ-bonded CH_3 complexes.[2-4]

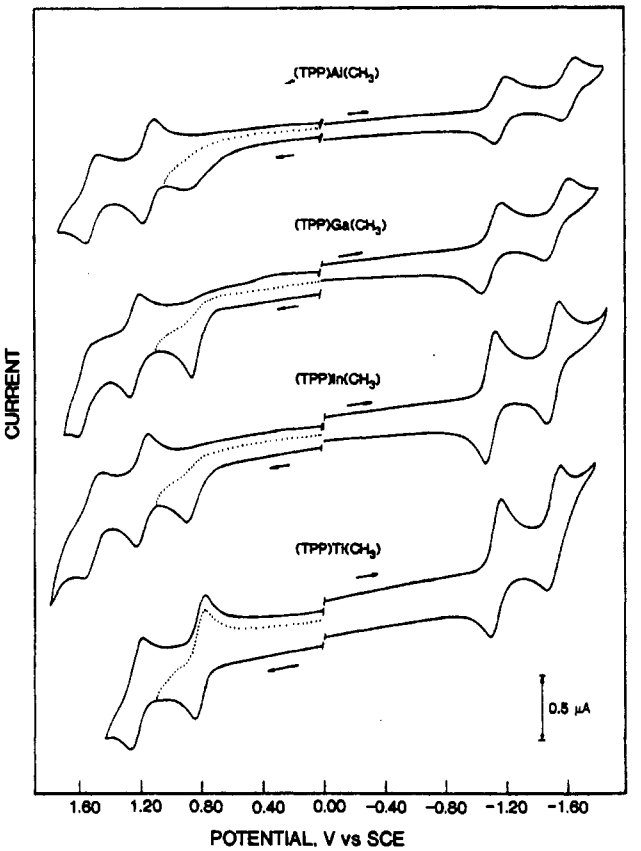

Figure 8. Cyclic voltammograms of (TPP)M(CH_3) in PhCN, 0.1 M TBA(PF_6), where M = Al, Ga, In, or Tl. Scan rate = 0.1 V s^{-1}.

In contrast, a cleavage of the metal–carbon bond does not occur for $[(OEP)Tl(CH_3)]^{\bullet+}$ or $[(TPP)Tl(CH)_3]^{\bullet+}$ and, in this case, two reversible oxidations are observed.[21]

In summary, the reduction of (P)Al(R) is similar to that of (P)Ga(R), (P)In(R), and (P)Tl(R). In contrast the oxidation of (P)Al(R) is similar to that of (P)Ga(R) and (P)In(R) but differs from that of (P)Tl(R). Each reduction of (TPP)Al(R) and (OEP)Al(R) is reversible, while the first oxidation of the same two complexes is irreversible and involves a cleavage of the Al–C σ bond. Peak potentials for the first oxidation of (OEP)Al(R) in PhCN, 0.1 M TBA(PF_6) vary between 0.71 and 0.76 V for a scan rate of 0.1 V s^{-1}, while E_p values for the first oxidation of (TPP)Al(R) vary between 0.80 and 0.88 V under the same experimental conditions. Linear relationships between the substituent constant of the σ-bonded R group and $E_{1/2}$ for either reduction or oxidation of (TPP)In(R) and (OEP)In(R) have been reported,[10] but no such correlations are obtained for the (P)Al(R) complexes in any of the three investigated solvent systems.

Acknowledgment. The support of the CNRS and the National Science Foundation (Grant CHE-8822881) is gratefully acknowledged.

Supplementary Material Available: Tables of crystallographic experimental conditions and least-squares refinement data, hydrogen atom fractional coordinates, anisotropic temperature factor expressions (U's), bond distances and angles in the porphyrin ligand, and least-squares planes (13 pages); a table of observed and calculated structure factors for (OEP)Al(CH_3) (27 pages). Ordering information is given on any current masthead page.